2023 62nd IEEE Conference on Decision and Control (CDC)
December 13-15, 2023. Marina Bay Sands, Singapore

Coordinated Control of Load Tap Changer Transformers for Voltage Regulation and Voltage Hunting Prevention: A Switched Systems Approach

Ismael Jaramillo[1], Ángel Mercado-Uribe[1] and Johannes Schiffer[1,2]

***Abstract*— We propose a coordinated control strategy for load tap changer (LTC) transformers in high voltage radial transmission systems that are connected to higher voltage grids and active distribution networks. We utilize switched systems modeling tools to capture the non-smooth characteristics of the LTCs. Our approach employs a state- and time-dependent switching logic to regulate the voltage at a specific node while preventing stability issues produced by the voltage hunting phenomenon. Then, we derive sufficient tuning conditions for the LTC control parameters, namely, deadband widths and time delays, as a function of the tap magnitude of the LTCs. These conditions ensure the existence of an exponentially stable equilibrium point of the closed-loop switched system and the exponential convergence of its output, *i.e.*, the regulated voltage, to a desired set. Finally, a numerical example shows the proposed strategy's superior performance over an uncoordinated scenario.**

I. INTRODUCTION

A load tap changer (LTC) is a motorized mechanical arrangement that adjusts the turns ratio of a transformer via discrete switches [1]. This type of device is employed for keeping the voltage at the lower-level substation side within acceptable limits [2]. For this purpose, the LTC compares local voltage measurements against a predefined setpoint and triggers tap switches after a certain time delay [1], [2]. In contrast to passive networks with unidirectional power flows, the interaction between distributed generators (DGs) within active distribution networks (ADNs) and LTCs can produce undesired phenomena due to the reversed power flows [3].

Voltage hunting is a highly detrimental phenomenon characterized by periodic oscillations around the voltage setpoint [4]. This adverse behavior can arise from conflicting interactions between DGs and LTCs and poses significant technical and economic threats, *e.g.*, damage of equipment, overactuation of the LTCs or cascading faults [5]. Motivated by this, coordinated control strategies for LTC-based voltage regulation and prevention of such (tap-induced) voltage hunting have been proposed in several papers [4], [5], [6].

Coordinated control strategies usually rely on tuning the LTC control parameters, *i.e.*, defining appropriate voltage deadbands and time delays. In [4], the voltage deadbands are defined based on the geographical location of the DGs and LTCs, while the time delays vary depending on the grid conditions. Similarly, the approach from [6] employs deadbands with adjustable thresholds and estimated voltage measurements. In a different setting, the authors of [5] parametrize the conditions that produce voltage hunting by analyzing the relationship between the tap magnitude, operation range and control parameters of LTCs. A common characteristic shared by this type of strategy is that no formal stability guarantees are provided.

In practice, LTC control strategies, *e.g.*, [4], [5], [6], produce both continuous and discrete dynamics. From a control systems perspective, this type of behavior can be described by employing modeling tools within the hybrid systems framework [7], see also [8]. A specific subset of hybrid systems, namely switched systems, offers effective methods for analyzing engineering systems with hybrid features [9], such as LTCs. Switched systems comprise a family of continuous subsystem dynamics together with a switching logic that orchestrates the discrete transitions between them [9]. Since the switching logic can be interpreted as a hybrid system [10], classic stability concepts for switched systems, *e.g.*, [11], [12], can be extended to general hybrid systems [7], [10]. However, a key advantage of the former methods is the reduced intricacy of the conditions required for guaranteeing stability properties [10].

A. Main contributions

From the above considerations, the contributions of the present paper are characterized by the following key features:

1) We provide a formal characterization of the voltage hunting phenomenon and derive a model for high voltage (HV) radial transmission grids that interface LTCs and DG-based ADNs by employing switched systems modeling tools. By using this approach, we are able to capture the non-smooth features of the LTCs. Compared to existing hybrid models, *e.g.*, [5], [8], stability guarantees can be derived in a less elaborate fashion due to the absence of discontinuities in the proposed system's solutions.
2) The coordinated control strategy is designed as a state- and time-dependent switching logic in which voltage deadbands and time delays serve as control parameters. Then, we derive sufficient tuning conditions for the control parameters, which ensure the existence of an

This work was supported by the German Research Foundation (Project no. 360332943).

Contact: {jaramism,mercadou,schiffer}@b-tu.de.
[1] Fachgebiet Regelungssysteme und Netzleittechnik, Brandenburgische Technische Universität Cottbus-Senftenberg.
[2] Fraunhofer Research Institution for Energy Infrastructures and Geothermal Systems (IEG), Cottbus.

exponentially stable equilibrium point of the closed-loop switched system and the exponential convergence of its output, *i.e.*, the regulated voltage, to a desired set, while preventing voltage hunting.

3) We provide a numerical example that illustrates the proposed control strategy's superior performance compared to an uncoordinated scenario.

B. Organization of the paper

This paper is organized as follows. In Section II, the dynamic model of the grid with uncoordinated LTCs is presented. Subsequently, in Section III, we introduce the proposed state- and time-dependent switching logic for the coordinated control strategy of the LTCs, derive the resulting closed-loop switched dynamics and formulate the problem statement. Based on this, our main results to address the considered problem are derived in Section IV. A numerical example for illustrating the theoretical results is provided in Section V and conclusions are drawn in Section VI.

C. Notation

We define the sets $\mathbb{Z} = \{\dots, -1, 0, 1, \dots\}$ and $\mathbb{T} = [0, 2\pi)$. For any $a \in \mathbb{R}$, $\mathbb{Z}_{\geq a} = \{x \in \mathbb{Z} | x \geq a\}$, $\mathbb{R}_{\geq a} = \{x \in \mathbb{R} | x \geq a\}$ and $\mathbb{R}_{\leq a} = \{x \in \mathbb{R} | x \leq a\}$. The cardinality of a closed set $\mathcal{A}$ is denoted by $|\mathcal{A}|$, while the minimum and maximum value of its elements are denoted by $\underline{\mathcal{A}}$ and $\overline{\mathcal{A}}$, respectively. The limit as t approaches a scalar $T \in \mathbb{R}$ from the right (correspondingly from the left) is denoted by t^+ (correspondingly t^-). The 2-norm of a vector $v \in \mathbb{R}^n$ is given by $\|v\| = \sqrt{v^\top v}$ and its distance with respect to a set $\mathcal{X} \subset \mathbb{R}^n$ is denoted by $\|v\|_{\mathcal{X}} = \min\{\|v - x\| | x \in \mathcal{X}\}$. Let $\mathbf{I}_n \in \mathbb{R}^{n \times n}$ denote the $n \times n$ identity matrix, $\text{diag}(a_{ii}) \in \mathbb{R}^{n \times n}$ a diagonal matrix with entries $a_{ii} \in \mathbb{R}$, $i = 1, \dots, n$, $a_{ij} \in \mathbb{R}$ the entry at the ith row and jth column of a matrix $A \in \mathbb{R}^{n \times n}$, $\|A\|$ its induced 2-norm and $\text{sgn}(c) \in \{-1, 0, 1\}$ the signum function, which returns the sign of $c \in \mathbb{R}$.

II. Considered system

In this section, we describe the type of power system employed for designing the proposed LTC coordinated control strategy. Namely, we focus on HV radial transmission grids involving ADNs, loads and LTCs. We consider an aggregated HV region of the Nordic test system [13] due to its adequacy for voltage stability studies, see [14], [15]. The considered HV grid is interfaced with an extra high voltage (EHV) substation and a medium voltage (MV) ADN composed of a MV DG and a HV load [16] via ideal LTCs, see Fig. 1.

A. Power system dynamics

We denote the set of grid nodes by $\mathcal{N} = \{1, 2, 3, 4\}$ and associate a phase angle $\delta_i(t) \in \mathbb{T}$ as well as a voltage amplitude $V_i(t) \in \mathbb{R}_{>0}$ to each node $i \in \mathcal{N}$ in the grid. Similarly to [17], we consider purely inductive transmission lines in the grid, *i.e.*, two nodes $i \in \mathcal{N}$, $j \in \mathcal{N}$, are connected via an inductive impedance $X_{ij} \in \mathbb{R}_{>0}$. For convenience, we define $X_{ij} = 0$ whenever i and j are not directly connected. The set of neighbors of a node $i \in \mathcal{N}$ is denoted by $\mathcal{N}_i := \{j | j \in \mathcal{N}, j \neq i, X_{ij} \neq 0\}$.

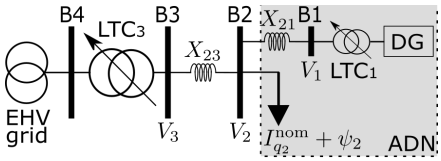

Fig. 1. Schematic diagram of the considered transmission grid. The voltage at bus B2 is regulated by a coordinated control strategy of LTC_1 and LTC_3. The considered ADN is shown in the shaded area.

Inspired by [4], [5], we design an LTC coordinated control strategy that aims at keeping[1] V_2 within acceptable limits, while preventing voltage hunting. To achieve this, we control the voltage at the jth LTC-controlled node V_j, $j \in \mathcal{N}_2 = \{1, 3\}$ and introduce the following assumption.

Assumption 1: $\delta_{ij} = \delta_i - \delta_j \approx 0$, $i \in \mathcal{N}$, $j \in \mathcal{N}_i$.

Assumption 1 is commonly known as the *standard decoupling approximation* and implies that the reactive power flows in the grid can be controlled via the node voltages [17]. With Assumption 1, the reactive power flow at the node of interest $Q_2 : \mathbb{R}_{>0}^{|\mathcal{N}|} \to \mathbb{R}$ is given by (cf. [17])

$$Q_2 = V_2(I_{q_2}^{\text{nom}} + \psi_2) = V_2^2 \sum_{j \in \mathcal{N}_2} \frac{1}{X_{2j}} - \sum_{j \in \mathcal{N}_2} \frac{V_2 V_j}{X_{2j}}, \quad (1)$$

where $I_{q_2}^{\text{nom}} \in \mathbb{R}$ is the nominal reactive current demand of the load and $\psi_2 \in \mathbb{R}$ is a constant current disturbance.

Available stability studies, *e.g.*, [14], [15], rely on the steady-state analysis of (1). However, the post-disturbance transient response of the LTCs requires a dynamical assessment [13]. It has been shown in [18] that the exponential recovery load model can describe the reactive current injection produced by the reactance variation associated to the LTC tap changes. Inspired by this, we define

$$\tau_{q_j} \frac{I_{q_j}}{dt} = -I_{q_j} + \frac{V_j - V_2}{X_{2j}}, \quad j \in \mathcal{N}_2, \quad (2)$$

where $I_{q_j} \in \mathbb{R}$ represents the reactive current injection of the jth LTC-controlled node into node B2, with time constant $\tau_{q_j} \in \mathbb{R}_{>0}$. Based on this, we can divide (1) by V_2, such that

$$V_2 = X_{q_2}\Big(\sum_{j \in \mathcal{N}_2} I_{q_j} + I_{q_2}^{\text{nom}} + \psi_2\Big), \; X_{q_2} = \frac{X_{21} X_{23}}{X_{21} + X_{23}}. \quad (3)$$

B. LTC actuation variables

In order to regulate V_2 in (3), V_j, $j \in \mathcal{N}_2$, can be controlled via its corresponding LTC switches [1], [3], *i.e.*,

$$V_j = V_j^{\text{nom}} + n_j v_j, \quad n_j \in [-\hat{n}_j, \hat{n}_j] \subset \mathbb{Z}, \hat{n}_j \in \mathbb{Z}_{>0}, \quad (4)$$

where $v_j \in \mathbb{R}_{>0}$, $j \in \mathcal{N}_2$, is the tap magnitude, n_j is the tap position, $\hat{n}_j$ is the maximum tap position and $V_j^{\text{nom}} \in \mathbb{R}_{>0}$ is the nominal voltage at the jth LTC-controlled node.

Next, we define the set $\Sigma = \{n_1, n_3\}$ and its possible permutations as

$$\sigma \in \mathcal{S} = \begin{cases} 1 & \text{for } \Sigma_1 = \{0, 0\}, \\ \vdots & \\ N & \text{for } \Sigma_N \neq \dots \neq \Sigma_2 \neq \Sigma_1, \end{cases} \quad (5)$$

[1] In order to simplify the notation, in the sequel, the time argument of all signals is omitted whenever clear from the context.

with $N = \Pi_{j\in\mathcal{N}_2}(2\hat{n}_j + 1) \in \mathbb{Z}_{>0}$ and $\Sigma_2, \ldots, \Sigma_{N-1}$ arbitrarily arranged. Hence, $\sigma \in \mathcal{S}$ represents the corresponding combination of LTC tap positions. Then, we define the nominal operation point of the considered system, as the solution of (2)-(3) with $\psi_2 = n_1 = n_3 = 0$ in (4), *i.e.*,

$$\begin{aligned} I_{q_j}^{\text{nom}} &= \frac{V_j^{\text{nom}} - X_{q_2}(I_{q_2}^{\text{nom}} + I_{q_i}^{\text{nom}})}{X_{q_2} + X_{2j}}, \\ V_2^{\text{nom}} &= X_{q_2}\sum_{k=1}^{3} I_{q_k}^{\text{nom}}, \end{aligned} \tag{6}$$

with X_{q_2} defined in (3) and $j \in \mathcal{N}_2$, $i \in \mathcal{N}_2 \setminus \{j\}$. Based on this, we introduce the desired deadband with acceptable limits around V_2^{nom} as the set

$$\mathcal{D}_1 = \{V_2 \in \mathbb{R}_{>0} | V_2^{\text{nom}} - \frac{\epsilon_1}{2} \leq V_2 \leq V_2^{\text{nom}} + \frac{\epsilon_1}{2}\}, \tag{7}$$

where the width $\epsilon_1 \in \mathbb{R}_{>0}$ is usually prescribed by the transmission system operators, *e.g.*, in [19].

III. LTC COORDINATION STRATEGY AND SWITCHED DYNAMICS

In this section, we introduce the switching logic that defines the proposed coordinated control strategy and derive resulting closed-loop switched dynamics. Similarly to [6], we employ an auxiliary deadband $\mathcal{D}_3 \subset \mathbb{R}$ defined as the set

$$\mathcal{D}_3 = \{V_2 \in \mathbb{R}_{>0} | V_2^{\text{nom}} - \frac{\epsilon_3}{2} \leq V_2 \leq V_2^{\text{nom}} + \frac{\epsilon_3}{2}\}, \tag{8}$$

where $\epsilon_3 > \epsilon_1$, with ϵ_1 given in (7). In addition, we consider a minimum time delay $\tau_{d_j} \in \mathbb{R}_{>0}$, $j \in \mathcal{N}_2$, between any consecutive switches of the jth LTC, see [4], [5].

Based on this, for any $V_2 \notin \mathcal{D}_1$, the LTCs must restore $V_2 \in \mathcal{D}_1$ via a coordinated switching strategy for n_j, $j \in \mathcal{N}_2$. To this purpose, we propose the following switching logic

$$n_j(t^+) = \begin{cases} n_j(t^-) - 1, & \text{if } V_2(t_d) \notin \mathcal{D}_1 \forall t_d \in [t - \tau_{d_j}, t) \\ & \text{and } V_2(t^-) > \overline{\mathcal{D}}_j, \\ n_j(t^-) + 1, & \text{if } V_2(t_d) \notin \mathcal{D}_1 \forall t_d \in [t - \tau_{d_j}, t) \\ & \text{and } V_2(t^-) < \underline{\mathcal{D}}_j, \end{cases} \tag{9}$$

with control parameters $\tau_{d_3} > \tau_{d_1}$ and $\epsilon_3 > \epsilon_1$. Hence, the discontinuous behavior of $\sigma(t)$ can be summarized as

$$\sigma(t) = \begin{cases} \sigma(t) \in \mathcal{S} & \text{if } t^k \leq t < t^{k+1}, \\ s \in \mathcal{S} & \text{if } t \geq t^{k+1} \text{ and } \Sigma_{\sigma(t)} = \Sigma_s, \end{cases} \tag{10}$$

where $t^k \in \mathbb{R}_{>0}$ is the time at which the kth switch is imposed, with $k \in \mathbb{Z}_{>0}$ and Σ_σ is defined in (5).

In order to derive the closed-loop switched dynamics produced by imposing (10) on (2),(3), let

$$x = \begin{bmatrix} I_{q_1} & I_{q_3} \end{bmatrix}^\top \in \mathbb{R}^2, \quad \kappa_{\sigma(t)} = \begin{bmatrix} n_1(t) & n_3(t) \end{bmatrix}^\top \in \mathbb{Z}^2,$$

where $\kappa_{\sigma(t)}$, $\sigma(t) \in \mathcal{S}$, is a piecewise constant control law, which switches according to (10). Then, the resulting closed-loop switched dynamics can be written as

$$\begin{aligned} \dot{x} &= Ax + B\kappa_{\sigma(t)} + b, \\ y &= V_2 = Cx + X_{q_2}(I_{q_2}^{\text{nom}} + \psi_2), \end{aligned} \tag{11}$$

where $y \in \mathbb{R}$ is the system output, with $C = X_{q_2}\begin{bmatrix} 1 & 1 \end{bmatrix}$ and

$$A = \begin{bmatrix} -\frac{1+\frac{X_{q_2}}{X_{21}}}{\tau_{q_1}} & -\frac{X_{q_2}}{\tau_{q_1}X_{21}} \\ -\frac{X_{q_2}}{\tau_{q_3}X_{23}} & -\frac{1+\frac{X_{q_2}}{X_{23}}}{\tau_{q_3}} \end{bmatrix}, \quad B = \begin{bmatrix} \frac{v_1}{\tau_{q_1}X_{21}} & 0 \\ 0 & \frac{v_3}{\tau_{q_3}X_{23}} \end{bmatrix},$$

$$b = \begin{bmatrix} \frac{V_1^{\text{nom}} - X_{q_2}(I_{q_2}^{\text{nom}} + \psi_2)}{\tau_{q_1}X_{21}} & \frac{V_3^{\text{nom}} - X_{q_2}(I_{q_2}^{\text{nom}} + \psi_2)}{\tau_{q_3}X_{23}} \end{bmatrix}^\top.$$

A. Voltage hunting definition and problem statement

Denote a switching sequence imposed by (10), as

$$\Omega = \{\sigma(t^{k_+}) \in \mathcal{S} | k \in \mathbb{Z}_{>0}\}, \tag{12}$$

where $t^{k+1} - t^k \geq \tau_d^k \in \mathbb{R}_{>0}$, for all t^k. Based on [8], the voltage hunting phenomenon is characterized by a switching sequence Ω that produces overcompensation of V_2 around $\mathcal{D}_1$ in (7), *i.e.*, there exists a non-empty set

$$\begin{aligned} \mathcal{H} = \{\sigma(t^{k_+}) \in \Omega | &\text{sgn}(V_2(t^k) - \phi(t^k)) \neq \\ &\text{sgn}(V_2(t^k + \tau_d^k) - \phi(t^k))\}, \end{aligned} \tag{13}$$

where $\phi(t^k)$ denotes the furthest point $\nu \in \mathcal{D}_1$ with respect to $V_2(t^k)$, given by

$$\phi(t^k) = \begin{cases} V_2^{\text{nom}} + \frac{\epsilon_1}{2} & \text{if } V_2(t^k) < \underline{\mathcal{D}}_1 = V_2^{\text{nom}} - \frac{\epsilon_1}{2}, \\ V_2^{\text{nom}} - \frac{\epsilon_1}{2} & \text{if } V_2(t^k) > \overline{\mathcal{D}}_1 = V_2^{\text{nom}} + \frac{\epsilon_1}{2}. \end{cases} \tag{14}$$

Definition 1: If Ω in (12) produces $|\mathcal{H}| > 1$ in (13), the system (11) exhibits voltage hunting.

Problem 1: Consider the system (11). Derive conditions for ψ_2 and ϵ_1, and design the control parameters of (9), τ_{d_1}, τ_{d_3} and ϵ_3, for ensuring that any switching sequence Ω imposed by the switching logic (10) prevents voltage hunting and guarantees that for any $\sigma(t^0) \in \mathcal{S}$, there exists $T \in \mathbb{R}_{>0}$, such that $y(t) \in \mathcal{D}_1$ for all $t \geq T$ and there exists an exponentially stable equilibrium point of the closed-loop switched dynamics.

IV. TUNING CONDITIONS FOR COORDINATED LTC CONTROL

In this section, we introduce the dynamic characteristics of the switched system (11), which are relevant for addressing Problem 1. Based on these, we tackle the problem of voltage hunting prevention and subsequently, we address the problem of existence of equilibria and their stability.

A. Voltage hunting prevention

From (5), each combination $\Sigma_\sigma = \{n_1, n_3\}$, $\sigma \in \mathcal{S}$, implies that the corresponding subsystem dynamics in (11) has an equilibrium point given by

$$\begin{aligned} x^{\star_\sigma} &= -A^{-1}\Theta_\sigma, \quad \Theta_\sigma = B\kappa_\sigma + b, \\ y^{\star_\sigma} &= Cx^{\star_\sigma} + X_{q_2}(I_{q_2}^{\text{nom}} + \psi_2). \end{aligned} \tag{15}$$

By solving the matrix multiplication $-CA^{-1}(B\kappa_\sigma + b)$ for $y^{\star_\sigma}$ in (15) and using the notion of $I_{q_j}^{\text{nom}}$, $j \in \mathcal{N}_2$, introduced

in (6), we can rewrite $y^{\star_\sigma}$ as

$$\begin{aligned} y^{\star_\sigma} &= -CA^{-1}(B\kappa_\sigma + b) + X_{q_2}(I_{q_2}^{\text{nom}} + \psi_2) \\ &= X_{q_2}\left(\sum_{k=1}^{3} I_{q_k}^{\text{nom}} + \frac{\psi_2}{2} + \sum_{j\in\mathcal{N}_2}\frac{n_j v_j}{2X_{2j}}\right) \\ &= V_2^{\text{nom}} + \frac{X_{q_2}\psi_2}{2} + \sum_{j\in\mathcal{N}_2} n_j\Delta_j, \quad \Delta_j = \frac{X_{q_2}v_j}{2X_{2j}}. \end{aligned} \tag{16}$$

Next, we compute the solution $x(t)$ of (11), during any time interval $t \in [t^{k-1}, t^k)$, $k \geq 1$, which is given by (cf. [20])

$$x(t^{k-1}+\bar{t}) = e^{A\bar{t}}x(t^{k-1}) + \int_0^{\bar{t}} e^{A(\bar{t}-T)}\Theta_{\sigma(t^{k-1_+})}dT,$$

where $0 \leq \bar{t} < t^k - t^{k-1}$ and $\Theta_{\sigma(t^{k-1_+})}$ defined in (15) is constant between switches, *i.e.*, during $t \in [t^{k-1}, t^k)$. By solving the integral part of this expression, we obtain

$$x(t^{k-1}+\bar{t}) = e^{A\bar{t}}x(t^{k-1}) + \left(\mathbf{I}_2 - e^{A\bar{t}}\right)x^{\star_{\sigma(t^{k-1_+})}}, \tag{17}$$

where $x^{\star_{\sigma(t^{k-1_+})}} = -A^{-1}\Theta_{\sigma(t^{k-1_+})}$ is the equilibrium point of the active subsystem dynamics, given in (15). Subtracting $x^{\star_{\sigma(t^{k-1_+})}}$ on both sides of (17) and premultiplying by C, yields

$$y(t^{k-1}+\bar{t}) - y^{\star_{\sigma(t^{k-1_+})}} = Ce^{A\bar{t}}\chi(t^{k-1}), \tag{18}$$

with $y^{\star_{\sigma(t^{k-1_+})}}$ given in (15) and where we used the shorthand $\chi(t^{k-1}) = x(t^{k-1}) - x^{\star_{\sigma(t^{k-1_+})}}$, such that

$$\|y(t^{k-1}+\bar{t}) - y^{\star_{\sigma(t^{k-1_+})}}\| \leq \|C\|\|e^{A\bar{t}}\|\|\chi(t^{k-1})\|. \tag{19}$$

Assumption 2: There exists[2] $I_{\max} \in \mathbb{R}_{>0}$, such that $\|x(t^0)\| \leq I_{\max}$ and $\max_{\sigma\in\mathcal{S}}\|x^{\star_\sigma}\| \leq I_{\max}$.

Lemma 1: The matrix A in (11) is Hurwitz with eigenvalues $\lambda_1(A) \in \mathbb{R}_{<0}$ and $\lambda_2(A) \in \mathbb{R}_{<0}$, $\lambda_1(A) \neq \lambda_2(A)$.

Proof: The eigenvalues of A are given by

$$\lambda_i(A) = \frac{a_{11}+a_{22} \pm \sqrt{(a_{11}-a_{22})^2 + 4a_{12}a_{21}}}{2}, \tag{20}$$

with $i = 1, 2$. Since all entries $a_{ik} < 0$, $i = 1, 2$, $k = 1, 2$, of A in (11), $(a_{11}-a_{22})^2 + 4a_{12}a_{21} > 0 > a_{11}+a_{22}$ in (20). Hence, $\sqrt{(a_{11}-a_{22})^2 + 4a_{12}a_{21}} \in \mathbb{R}_{>0}$, *i.e.*, $\lambda_1(A) \in \mathbb{R}$ and $\lambda_2(A) \in \mathbb{R}$. Moreover, the numerator of (20) satisfies

$$(a_{11}+a_{22})^2 - \left(\sqrt{(a_{11}-a_{22})^2 + 4a_{12}a_{21}}\right)^2 = \tfrac{8}{\tau_{q_1}\tau_{q_3}} > 0,$$

which implies that

$$|a_{11}+a_{22}| > |\sqrt{(a_{11}-a_{22})^2 + 4a_{12}a_{21}}|.$$

Then, $\max\{a_{11}+a_{22} \pm \sqrt{(a_{11}-a_{22})^2 + 4a_{12}a_{21}}\} < 0$ and A is Hurwitz, with $\lambda_1(A) \neq \lambda_2(A)$. ∎

Lemma 1 implies that there exist matrices $\Lambda \in \mathbb{R}^{2\times 2}$ and $W \in \mathbb{R}^{2\times 2}$, such that (cf. [21, Ch. 3.5])

$$\Lambda = \text{diag}(\lambda_i(A)) = W^{-1}AW, \quad W = \begin{bmatrix}\mathbf{v}_1 & \mathbf{v}_2\end{bmatrix}, \tag{21}$$

where $\mathbf{v}_i \in \mathbb{R}^{2\times 1}$, $i = 1, 2$, is the eigenvector associated to the ith $\lambda_i(A)$, given in (20). Based on this, we can establish

$$\|e^{A\bar{t}}\| = \|W\|\|e^{\Lambda\bar{t}}\|\|W^{-1}\| \leq \zeta e^{-\varepsilon\bar{t}}, \tag{22}$$

[2]From a practical perspective, Assumption 2 prevents that $x(t^0)$ and $x^{\star_\sigma}$ in (15) violate any current protection limits, see, *e.g.*, [19].

with $\zeta = \max_{i,k}\sqrt{\lambda_i(WW^\top)\lambda_k(W^{-1}(W^{-1})^\top)} \in \mathbb{R}_{>1}$ and $\varepsilon = \min_i|\lambda_i(A)| \in \mathbb{R}_{>0}$.

Note that all subsystem dynamics $\sigma \in \mathcal{S}$ in (11) share the same system matrix A. Since A is Hurwitz, for every time interval $t \in [t^{k-1}, t^k)$, $k \geq 1$, with $t^k > t^{k-1} + \bar{t} \geq t^{k-1} \geq t^0$, we can use Assumption 2 together with (17) and the triangle inequality to obtain

$$\begin{aligned} \|\chi(t^{k-1}))\| &\leq \max_{\sigma\in\mathcal{S}}\|x(t^0) - x^{\star_{\sigma(t^{k-1_+})}}\| \\ &\leq \max\|x(t^0)\| + \max_{\sigma\in\mathcal{S}}\|x^{\star_\sigma}\| \leq 2I_{\max}, \end{aligned} \tag{23}$$

with $\chi(t^{k-1})$ defined in (18). Hence, with (22), (23) and $\|C\| = \sqrt{2}X_{q_2}$ in (11), (19) can be upper-bounded as

$$\|y(t^{k-1}+\bar{t}) - y^{\star_{\sigma(t^{k-1_+})}}\| \leq 2\sqrt{2}X_{q_2}I_{\max}\zeta e^{-\varepsilon\bar{t}}. \tag{24}$$

Based on this notion, the problem of voltage hunting prevention is addressed in the following lemma.

Lemma 2: Consider the dynamics (11) with switching logic (10) and Assumption 2. For any given Δ_1 and Δ_3 in (16), if $\epsilon_1 \geq 2\Delta_1$ and the control parameters of (9) are chosen according to

$$\begin{aligned} &\tau_{d_1} > \frac{\log(\mu(\upsilon))}{\varepsilon}, \quad \mu(\upsilon) = \frac{2\sqrt{2}X_{q_2}I_{\max}\zeta}{\upsilon}, \\ &\tau_{d_3} = c\tau_{d_1}, \quad c \in \mathbb{Z}_{>1}, \quad \epsilon_3 \geq \epsilon_1 + \Delta_3, \end{aligned} \tag{25}$$

with $\upsilon \in \mathbb{R}_{>0}$, $\upsilon < \Delta_1$, being a design parameter and $\zeta > 1$, $\varepsilon > 0$ given in (22), then any switching sequence Ω imposed by the switching logic (10) ensures that $|\mathcal{H}| \leq 1$, with $\mathcal{H}$ defined in (13). That is, voltage hunting is prevented, see Definition 1.

Proof: Since $\tau_{d_3} = c\tau_{d_1}$, with $c \in \mathbb{Z}_{>1}$, at any t^i, such that (9) imposes $n_3(t^{i-}) \neq n_3(t^{i_+})$, also $n_1(t^{i-}) \neq n_1(t^{i_+})$. Hence, $t^k - t^{k-1} \geq \tau_{d_1}$, for all $k \geq 1$ in (10). Based on this, the proof is split into two parts.

First, inspired by [22], we design τ_{d_1} for ensuring that any switch $\sigma(t^{k_+}) \neq \sigma(t^{k-1_+})$, $k \geq 1$, can only occur if $y(t^{k-1}+\tau_{d_1})$ has reached a neighborhood of $y^{\star_{\sigma(t^{k-1_+})}}$. Hence, with Assumption 2 and (24), we seek to impose

$$\|y(t^{k-1}+\tau_{d_1}) - y^{\star_{\sigma(t^{k-1_+})}}\| \leq 2\sqrt{2}X_{q_2}I_{\max}\zeta e^{-\varepsilon\tau_{d_1}} < \upsilon, \tag{26}$$

for some design parameter $\upsilon > 0$ to be specified in the second part of the proof. Solving for τ_{d_1}, yields

$$\tau_{d_1} > \frac{\log(\mu(\upsilon))}{\varepsilon}, \quad \mu(\upsilon) = \frac{2\sqrt{2}X_{q_2}I_{\max}\zeta}{\upsilon}.$$

In the second part of the proof, we derive sufficient conditions for υ, ϵ_1 and ϵ_3, which ensure $|\mathcal{H}| \leq 1$. From (9) and (16), every switch $\sigma(t^{k_+}) \in \Omega$ produces

$$|y^{\star_{\sigma(t^{k_+})}} - y^{\star_{\sigma(t^{k-1_+})}}| \in \begin{cases}\{\Delta_1, \Delta_1+\Delta_3\} & \text{if } y(t^k) \notin \mathcal{D}_3, \\ \{\Delta_1\} & \text{if } y(t^k) \in \mathcal{D}_3.\end{cases} \tag{27}$$

Based on this, set $\upsilon < \Delta_1$. Moreover, let $\Omega = \Omega_1 \cup \Omega_3$ in (12), with $\Omega_1 \subseteq \Omega$ and $\Omega_3 \subseteq \Omega$, $\Omega_1 \cap \Omega_3 = \emptyset$, such that $\sigma(t^{i_+}) \in \Omega_1$ and $\sigma(t^{l_+}) \in \Omega_3$ represent the switches occurring when $y(t^i) \in \mathcal{D}_3$ and $y(t^l) \notin \mathcal{D}_3$, respectively. Then, consider any extreme scenario where $y^{\star_{\sigma(t^{i-1_+})}} \notin \mathcal{D}_1$ and $y^{\star_{\sigma(t^{l-1_+})}} \notin \mathcal{D}_3$ are arbitrarily close to $\mathcal{D}_1$ and $\mathcal{D}_3$,

respectively, *i.e.*,

$$0 < \|y^{\star}{}^{\sigma(t^{i^{-1}+})}\|_{\mathcal{D}_1} = \gamma_1, \quad 0 < \|y^{\star}{}^{\sigma(t^{l^{-1}+})}\|_{\mathcal{D}_3} = \gamma_3,$$

with $0 < \gamma_j < \Delta_1 - \upsilon$, $j \in \mathcal{N}_2$, and[3] $y^{\star}{}^{\sigma(t^{l^{-1}+})} < \underline{\mathcal{D}}_3 \leq y^{\star}{}^{\sigma(t^{i^{-1}+})} < \underline{\mathcal{D}}_1$. Based on this, we seek to prove that $\Omega_1 \cap \mathcal{H} = \emptyset$ and $|\Omega_3 \cap \mathcal{H}| \leq 1$, for any Ω in (12). From $\mathcal{H}$ in (13), this implies that $\sigma(t^{i+}) \in \Omega_1$ and $\sigma(t^{l+}) \in \Omega_3$ produce $y(t^i + \tau_{d_1}) \in \mathcal{D}_1$ and $y(t^l + \tau_{d_1}) \in \mathcal{D}_3$, respectively. From (26) with $\upsilon < \Delta_1$ and (27), this is achieved if $y^{\star}{}^{\sigma(t^{i+})}$ and $y^{\star}{}^{\sigma(t^{l+})}$ given in (16), are upper-bounded by

$$\begin{aligned} y^{\star}{}^{\sigma(t^{i+})} &= y^{\star}{}^{\sigma(t^{i^{-1}+})} + \Delta_1 = V_2^{\text{nom}} - \frac{\epsilon_1}{2} - \gamma_1 + \Delta_1 \\ &\leq \overline{\mathcal{D}}_1 - \Delta_1 = V_2^{\text{nom}} + \frac{\epsilon_1}{2} - \Delta_1, \\ y^{\star}{}^{\sigma(t^{l+})} &\leq y^{\star}{}^{\sigma(t^{l^{-1}+})} + \Delta_1 + \Delta_3 \\ &= V_2^{\text{nom}} - \frac{\epsilon_3}{2} - \gamma_3 + \Delta_1 + \Delta_3 \\ &\leq \overline{\mathcal{D}}_3 - \Delta_1 = V_2^{\text{nom}} + \frac{\epsilon_3}{2} - \Delta_1, \end{aligned} \tag{28}$$

thus implying that ϵ_1 and ϵ_3 must satisfy

$$\epsilon_1 \geq 2\Delta_1 > 2\Delta_1 - \gamma_1, \quad \epsilon_3 \geq \Delta_3 + \epsilon_1 > \Delta_3 + 2\Delta_1 - \gamma_3.$$

Then, for any $\|y^{\star}{}^{\sigma(t^{i^{-1}+})}\|_{\mathcal{D}_1} \geq \gamma_1$ and $\|y^{\star}{}^{\sigma(t^{l^{-1}+})}\|_{\mathcal{D}_3} \geq \gamma_3$, (26)-(28) ensure that each $\sigma(t^{k+}) \in \Omega$, $k \geq 1$, imposed by (10) satisfies exactly one of the following scenarios:

1) $\sigma(t^{i+}) \in \Omega_1$. From $\phi(t^i)$ in (14), $\text{sgn}(y(t^i) - \phi(t^i)) = \text{sgn}(y(t^i + \tau_{d_1}) - \phi(t^i))$ and thus, $\Omega_1 \cap \mathcal{H} = \emptyset$, see (13).
2) $\sigma(t^{\ell+}) \in \Omega_3$, such that $y(t^\ell + \tau_{d_1}) \in \mathcal{D}_3$. From scenario 1), any possible subsequent switch, $\sigma(t^{k+})$, $t^k \geq t^\ell + \tau_{d_1}$, occurs when $y(t^k) \in \mathcal{D}_3 \setminus \mathcal{D}_1$. Thus, $\sigma(t^{k+}) \in \Omega_1$ and Ω in (12) contains at most, one $\sigma(t^{\ell+})$.
3) $\sigma(t^{p+}) \in \Omega_3 \setminus \{\sigma(t^{\ell+})\}$, *i.e*, $y(t^p + \tau_{d_1}) \notin \mathcal{D}_3$. From $\phi(t^p)$ in (14), $\text{sgn}(y(t^p) - \phi(t^p)) = \text{sgn}(y(t^p + \tau_{d_1}) - \phi(t^p))$ and thus, $(\Omega_3 \setminus \{\sigma(t^{\ell+})\}) \cap \mathcal{H} = \emptyset$, see (13).

From these scenarios, any Ω in (12) imposed by (10) has the form

$$\Omega = \{\sigma(t^{1+}), \ldots, \sigma(t^{p+}), \sigma(t^{\ell+}), \sigma(t^{i+}), \ldots\}, \tag{29}$$

with $t^p < t^\ell < t^i$, for any $\sigma(t^{p+}) \in \Omega_3 \setminus \{\sigma(t^{\ell+})\}$, $\sigma(t^{\ell+}) \in \Omega_3$ and $\sigma(t^{i+}) \in \Omega_1$. Then, $|\mathcal{H}| \leq \max\{|\emptyset|, |\{\sigma(t^\ell)\}|\} = 1$ and (10) prevents voltage hunting, see Definition 1. ■

B. Existence of equilibria and stability

Lemma 3: Consider the dynamics (11) with switching logic (10) and the set $\mathcal{D}_1$, defined in (7). If the constant disturbance ψ_2 in (1) satisfies $\psi_2 \in [-\hat{\psi}_2, \hat{\psi}_2]$, with

$$\hat{\psi}_2 = \sum_{j \in \mathcal{N}_2} \left(\frac{2\hat{n}_j \Delta_j}{X_{q_2}} \right) + \frac{\epsilon_1}{X_{q_2}}, \tag{30}$$

and $\hat{n}_j$ given in (4), then there exists a non-empty set $\mathcal{S}^\star \subset \mathcal{S}$, such that for every $s \in \mathcal{S}^\star$, $x^{\star s}$ given in (15) qualifies as an equilibrium point of the switched dynamics (11).

Proof: Any admissible equilibrium point $x^{\star s}$ must be such that

$$\dot{x}^{\star s}(t) = A x^{\star s} + B\kappa_s + b = 0 \quad \forall t \geq t^0, s \in \mathcal{S}^\star,$$

with κ_s being fixed for all $t \geq t^0$, *i.e.*, no LTC switches occur. From (9), this is achieved if and only if

$$\underline{\mathcal{D}}_1 \leq C x^{\star s} + X_{q_2}(I_{q_2}^{\text{nom}} + \psi_2) = y^{\star s} \leq \overline{\mathcal{D}}_1, \tag{31}$$

with $\underline{\mathcal{D}}_1$, $\overline{\mathcal{D}}_1$ defined in (7) and C given in (11). By substituting (16) in (31) and solving for ψ_2, we obtain

$$-\sum_{j \in \mathcal{N}_2} \left(\frac{2\hat{n}_j \Delta_j}{X_{q_2}} \right) - \frac{\epsilon_1}{X_{q_2}} \leq \psi_2 \leq \sum_{j \in \mathcal{N}_2} \left(\frac{2\hat{n}_j \Delta_j}{X_{q_2}} \right) + \frac{\epsilon_1}{X_{q_2}},$$

due to $n_j \in [-\hat{n}_j, \hat{n}_j]$ in (4). From (31), any $x(t^0) = x^{\star s}$, $s \in \mathcal{S}^\star \subset \mathcal{S}$, produces $\dot{x}^{\star s}(t) = 0$, for all $t \geq t^0$ and thus, $x^{\star s}$ qualifies as an equilibrium point of (11). ■

We are now in the position of presenting our main result.

Theorem 1: Let the conditions in Lemma 2 be satisfied and assume that $\psi_2 \in [-\hat{\psi}_2, \hat{\psi}_2]$, with $\hat{\psi}_2$ satisfying (30). Then, for any $\sigma(t^0) \in \mathcal{S}$, the switching logic (10) imposes a switching sequence $\Omega = \{\sigma(t^{1+}), \ldots, \sigma(t^{r+})\}$, which ensures that $y(t) \in \mathcal{D}_1$, for all $t \geq t^r + \tau_{d_1}$ and $x^{\star}{}^{\sigma(t^{r+})}$ is an exponentially stable equilibrium point of the switched dynamics (11), for some $\sigma(t^{r+}) \in \mathcal{S}^\star$.

Proof: Since $\mathcal{D}_1 \subset \mathcal{D}_3$, (26)-(28) ensure that any switching sequence Ω of the form (29) produces

$$\|y(t^k + \tau_{d_1})\|_{\mathcal{D}_1} - \|y(t^k)\|_{\mathcal{D}_1} < 0 \quad \forall k \geq 1. \tag{32}$$

From Lemma 3, there exists a set $\mathcal{S}^\star$, $|\mathcal{S}^\star| \geq 1$, such that for every $s \in \mathcal{S}^\star$, $y^{\star s} \in \mathcal{D}_1$. Hence, (32) implies that there exists $\sigma(t^{r+}) \in \Omega$, such that $\|y(t^r)\|_{\mathcal{D}_1} > \|y(t^r + \tau_{d_1})\|_{\mathcal{D}_1} = 0$. That is, $y(t^r + \tau_{d_1}) \in \mathcal{D}_1$. Therefore, (9) prevents any further switching for $t \geq t^r + \tau_{d_1}$ and thus, (26) yields

$$\lim_{\bar{t} \to \infty} \|y(t^r + \bar{t}) - y^{\star}{}^{\sigma(t^{r+})}\| = \lim_{\bar{t} \to \infty} 2\sqrt{2} X_{q_2} I_{\max} \zeta e^{-\varepsilon \bar{t}} = 0,$$

such that $y(t) \in \mathcal{D}_1$, for all $t \geq t^r + \tau_{d_1}$.

Finally, consider t^r in (17), subtract $x^{\star}{}^{\sigma(t^{r+})}$ and compute the norm on both sides of the equation. Based on this, we can conclude that

$$\lim_{\bar{t} \to \infty} \|x(t^r + \bar{t}) - x^{\star}{}^{\sigma(t^{r+})}\| = \lim_{\bar{t} \to \infty} \|e^{A\bar{t}}\| \|\chi(t^r)\| = 0,$$

with $\chi(t^r) = x(t^r) - x^{\star}{}^{\sigma(t^{r+})}$, due to A being Hurwitz, see Lemma 1. Then, $x^{\star}{}^{\sigma(t^{r+})}$, $\sigma(t^{r+}) \in \mathcal{S}^\star$, is an exponentially stable equilibrium point of the switched dynamics (11). ■

V. Numerical example

In this section, we compare the performance of the coordinated control strategy (9) against an uncoordinated scenario, via a simulation example conducted in MATLAB.

Scenario setup: We consider the grid in Fig. 1 with parameters summarized in Table I. The electrical parameters are taken from [13], while the thresholds of the deadband $\mathcal{D}_1$ are extracted from the German grid codes [19]. Inspired by [4], we employ fast reactive current time constants τ_{q_1}, τ_{q_3} and consider $I_{\max} = 1.1$ p.u., $\Delta_1 = 0.02$ p.u, $\Delta_3 = 0.07$ p.u and a disturbance $\psi_2 < 0$ in the reactive current demand of the load. Then, we set τ_{d_1} and τ_{d_3} according to (25).

Coordinated vs. uncoordinated LTC control strategy: The performance comparison is shown in Fig. 2. Due to the voltage drop produced by ψ_2, the LTC logic imposes a switch of n_1 at $t_1 = 1.2$ s to raise the voltage. Since $V_2(t_2) \notin \mathcal{D}_1$ at $t_2 = 2.2$ s, the uncoordinated control

[3] Since the sets $\mathcal{D}_j$, $j \in \mathcal{N}_2$, are symmetric around V_2^{nom}, the proof is analogous for any $y^{\star}{}^{\sigma(t^{l^{-1}+})} > \overline{\mathcal{D}}_3 \geq y^{\star}{}^{\sigma(t^{i^{-1}+})} > \overline{\mathcal{D}}_1$.

TABLE I

ELECTRICAL PARAMETERS OF THE CONSIDERED GRID.

Parameter	Value
$\boxed{X_{21} \;\; X_{23}}$	$\boxed{50.7 \;\; 47.32}$ Ω
$\mathcal{D}_1$	$\{0.98 \leq V_2 \leq 1.02\}$ p.u
$\boxed{\tau_{q_1} \;\; \tau_{q_3} \;\; \tau_{d_1} \;\; \tau_{d_3}}$	$\boxed{0.1 \;\; 0.05 \;\; 1 \;\; 2}$ s

scheme imposes simultaneous switches of n_1 and n_3. This behavior produces overcompensation and sustained periodic oscillations associated with voltage hunting. Alternatively, we propose a coordination strategy (9) with an auxiliary deadband $\mathcal{D}_3 = \{0.945 \leq V_2 \leq 1.055\}$. Under this setting, the switch of n_3 that produces overcompensation at t_2 is inhibited due to $V_2(t_2) \in \mathcal{D}_3 \setminus \mathcal{D}_1$. As a result, V_2 is restored to $\mathcal{D}_1$ shortly after t_2.

VI. CONCLUSIONS

We designed a coordinated control strategy for LTCs in a particular type of radial transmission grids, which is effective in regulating the voltage at a specific node and preventing voltage hunting. To capture the non-smooth LTC behavior, we employed switched systems modeling tools and designed a state- and time-dependent switching logic. Unlike related studies in the literature, *e.g.*, [4], [5], [6], we provided a formal characterization of the voltage hunting phenomenon and a formal stability analysis of the resulting closed-loop switched system. For the latter, we derived sufficient conditions for the voltage deadbands and time delays of the LTC control strategy, which ensure the existence of an exponentially stable equilibrium point of the closed-loop switched dynamics, such that the system's output converges to a desired set, while preventing voltage hunting. Finally, the practical advantages of the proposed control strategy over an uncoordinated scenario have been illustrated via a numerical example.

Based on these results, many interesting future research directions can be foreseen. For example, extending the present result to larger transmission grids, consider a broader spectrum of grid architectures or including the continuous dynamics of reactive power injection of DGs.

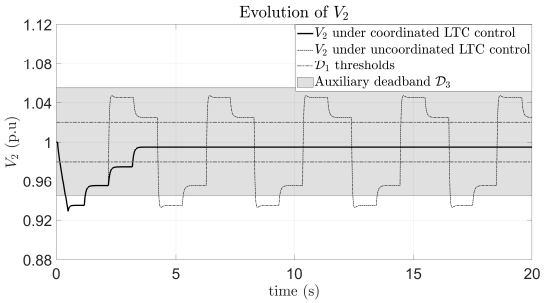

Fig. 2. V_2 performance at node B2 under the uncoordinated LTC operation (dotted line) and the proposed coordinated control strategy (solid line).

REFERENCES

[1] C. Gao and M. A. Redfern, "A review of voltage control techniques of networks with distributed generations using on-load tap changer transformers," in *International Univ. Power Eng. Conf.* IEEE, 2010, pp. 1–6.

[2] F. A. Viawan, A. Sannino, and J. Daalder, "Voltage control with on-load tap changers in medium voltage feeders in presence of distributed generation," *Electric Power Sys. Research*, vol. 77, no. 10, pp. 1314–1322, 2007.

[3] C. R. Sarimuthu, V. K. Ramachandaramurthy, K. Agileswari, and H. Mokhlis, "A review on voltage control methods using on-load tap changer transformers for networks with renewable energy sources," *Renew. and Sust. Energy Reviews*, vol. 62, pp. 1154–1161, 2016.

[4] K. M. Muttaqi, A. D. Le, M. Negnevitsky, and G. Ledwich, "A coordinated voltage control approach for coordination of OLTC, voltage regulator, and DG to regulate voltage in a distribution feeder," *IEEE Trans. on Industry App.*, vol. 51, no. 2, pp. 1239–1248, 2015.

[5] J. Swartz, F. Celi, F. Pasqualetti, and A. Von Meier, "Parameter conditions to prevent voltage oscillations caused by LTC-inverter hunting on power distribution grids," in *Eur. Control Conf.*, 2022, pp. 1118–1125.

[6] S. N. Salih and P. Chen, "On coordinated control of OLTC and reactive power compensation for voltage regulation in distribution systems with wind power," *IEEE Trans. on Power Sys.*, vol. 31, no. 5, pp. 4026–4035, 2015.

[7] C. Cai, A. R. Teel, and R. Goebel, "Smooth Lyapunov functions for hybrid systems-part I: Existence is equivalent to robustness," *IEEE Trans. on Autom. Control*, vol. 52, no. 7, pp. 1264–1277, 2007.

[8] V. Donde and I. A. Hiskens, "Analysis of tap-induced oscillations observed in an electrical distribution system," *IEEE Trans. on Power Sys.*, vol. 22, no. 4, pp. 1881–1887, 2007.

[9] H. Lin and P. J. Antsaklis, "Stability and stabilizability of switched linear systems: a survey of recent results," *IEEE Trans. on Autom. Control*, vol. 54, no. 2, pp. 308–322, 2009.

[10] R. Goebel, R. G. Sanfelice, and A. R. Teel, "Hybrid dynamical systems," *IEEE Control Sys. Magazine*, vol. 29, no. 2, 2009.

[11] J. P. Hespanha and A. S. Morse, "Stability of switched systems with average dwell-time," in *Conf. on Decision and Control*, 1999, pp. 2655–2660.

[12] A. S. Morse, "Supervisory control of families of linear set-point controllers-part I. Exact matching," *IEEE Trans. on Autom. Control*, vol. 41, no. 10, pp. 1413–1431, 1996.

[13] T. Van Cutsem, M. Glavic, W. Rosehart, J. Andrade dos Santos, C. Canizares, M. Kanatas, L. Lima, F. Milano, L. Papangelis, R. Andrade Ramos, B. Tamimi, G. Taranto, and C. Vournas, "Test systems for voltage stability analysis and security assessment," Tech. Rep., August 2015.

[14] L. Robitzky, D. Mayorga-Gonzalez, C. Kittl, C. Strunck, J. Zwartscholten, S. Muller, U. Hager, J. Myrzik, and C. Rehtanz, "Impact of active distribution networks on voltage stability of electric power systems," in *Bulk Power Sys. Dynamics and Control Symposium*, 2017, pp. 1–10.

[15] S. Liemann, L. Robitzky, and C. Rehtanz, "Impact of varying shares of distributed energy resources on voltage stability in electric power systems," in *PowerTech*. IEEE, 2019, pp. 1–6.

[16] W. R. E. M. T. Force, "WECC solar plant dynamic modeling guidelines," *See https://www.wecc. biz/Reliability/WECC Solar Plant Dynamic Modeling Guidelines. pdf*, 2014.

[17] J. Schiffer, T. Seel, J. Raisch, and T. Sezi, "Voltage stability and reactive power sharing in inverter-based microgrids with consensus-based distributed voltage control," *IEEE Trans. on Control Sys. Tech.*, vol. 24, no. 1, pp. 96–109, 2015.

[18] A. Arif, Z. Wang, J. Wang, B. Mather, H. Bashualdo, and D. Zhao, "Load modeling - a review," *IEEE Trans. on Smart Grid*, vol. 9, no. 6, pp. 5986–5999, 2017.

[19] V. VDE-AR-N, "4120: 2015-01 technical requirements for the connection and operation of customer installations to the high-voltage network (TCC high-voltage)," *VDE: Frankfurt am Main, Germany*, 2015.

[20] Z. Sun, S. S. Ge, and T. H. Lee, "Controllability and reachability criteria for switched linear systems," *Automatica*, vol. 38, no. 5, pp. 775–786, 2002.

[21] C. T. Chen, *Linear system theory and design*. Saunders college publishing, 1984.

[22] M. Dorothy and S.-J. Chung, "Switched systems with multiple invariant sets," *Systems and Control Letters*, vol. 96, pp. 103–109, 2016.